Supporting Information for "Robust and irreversible impacts of an AMOC collapse on tropical monsoon systems: a multi-model comparison"

M. Ben-Yami[1,2], P. Good[3], L. C. Jackson [3], M. Crucifix [4], A. Hu [5], O. Saenko [6], D. Swingedouw [7]and N. Boers [1,2,8]

[1]Earth System Modelling, School of Engineering and Design, Technical University of Munich, Munich, Germany

[2]Potsdam Institute for Climate Impact Research, Potsdam, Germany

[3]Met Office, Exeter, UK

[4]Earth and Life Institute, UCLouvain, Place Louis Pasteur 3, Louvain-La-Neuve, 1348, Belgium

[5]Climate and Global Dynamics Lab, National Center for Atmospheric Research, Boulder, CO 80307, USA

[6]SEOS, University of Victoria, BC, Canada

[7]Environnements et Paléoenvironnements Océaniques et Continentaux (EPOC)— Université de Bordeaux, Pessac, France

[8]Department of Mathematics and Global Systems Institute , University of Exeter, Exeter, UK

Contents of this file

Region	Longitude		Latitude	
	Min	Max	Min	Max
AM south	-75	-42.5	-15	-5
AM north	-75	-55	-5	5
WAM	-20	25	5	20
ISM	70	85	5	25
EASM	110	140	10	40

Table S1. Coordinates used to define the tropical monsoon boxes for Figure 4.

Region	Hosing	4xCO2	SSP585	SSP126
Global	0.66	0.65	0.66	0.60
60S-60N	0.66	0.57	0.58	0.51
Extratropics	0.49	0.74	0.68	0.62
Tropics	0.64	0.40	0.53	0.40
Southern AM	0.79	0.15	0.27	0.03
Northern AM	0.18	0.68	0.61	0.36
WAM	0.99	0.15	0.48	0.24
ISM	0.95	0.75	0.80	0.74
EASM	0.71	0.73	0.96	0.70

Table S2. Values from Figure 2a. Fraction of gridpoints in the respective region land areas where all four models of the experiments agree on the sign of mean annual precipitation anomaly. Extratropics are defined as 20S-60S and 20N-60N, and the tropics as 20S-20N, and the last five regions are as defined in Table S1. For the tropics and most monsoon regions there is more agreement in the hosing experiment than in the other experiments.

Region	Hosing	4xCO2	SSP585	SSP126
Global	0.35	0.52	0.49	0.33
60S-60N	0.42	0.41	0.39	0.26
Extratropics	0.33	0.56	0.49	0.33
Tropics	0.40	0.31	0.30	0.21
Southern AM	0.60	0.05	0.09	0.08
Northern AM	0.73	0.32	0.30	0.15
WAM	0.65	0.17	0.21	0.13
ISM	0.44	0.30	0.34	0.12
EASM	0.26	0.50	0.36	0.21

Table S3. Values from Figure 2b. Fraction of months in the respective region land areas where all four models of the experiments agree on the sign of mean monthly precipitation anomaly. Extratropics are defined as 20S-60S and 20N-60N, and the tropics as 20S-20N, and the last five regions are as defined in Table S1. For the tropics and most monsoon regions there is more agreement in the hosing experiment than in the other experiments.

Region	Longitude		Latitude	
	Min	Max	Min	Max
AM	-85	-30	-20	11
WAM	-20	35	-10	25
ISM	70	85	5	25
EASM	110	140	10	40

Table S4. Coordinates used to define the tropical monsoon regions for calculation of the dry and wet season in Figure 5.

Region	CanESM5			CESM2			IPSL		
	Cont	Weak	Diff	Cont	Weak	Diff	Cont	Weak	Diff
AM	0.59	0.83	0.68	0.54	0.74	0.67	0.69	0.84	0.69
WAM	0.90	0.93	0.88	0.91	0.88	0.88	0.81	0.90	0.77
ISM	0.81	0.85	0.62	0.89	0.88	0.65	0.39	0.47	-0.09
EASM	0.82	0.81	0.73	0.83	0.86	0.75	0.44	0.16	-0.00

Table S5. Correlation of precipitation of the CanESM5, CESM2, and IPSL models with HadGEM. The table shows Pearson's correlation coefficient of the time-averaged precipitation patterns in the four regions between HadGEM and the three other models, for the piControl (Cont) and weak AMOC (Weak) runs, as well as the difference between them (Diff). The regions are defined as in Figure 5.

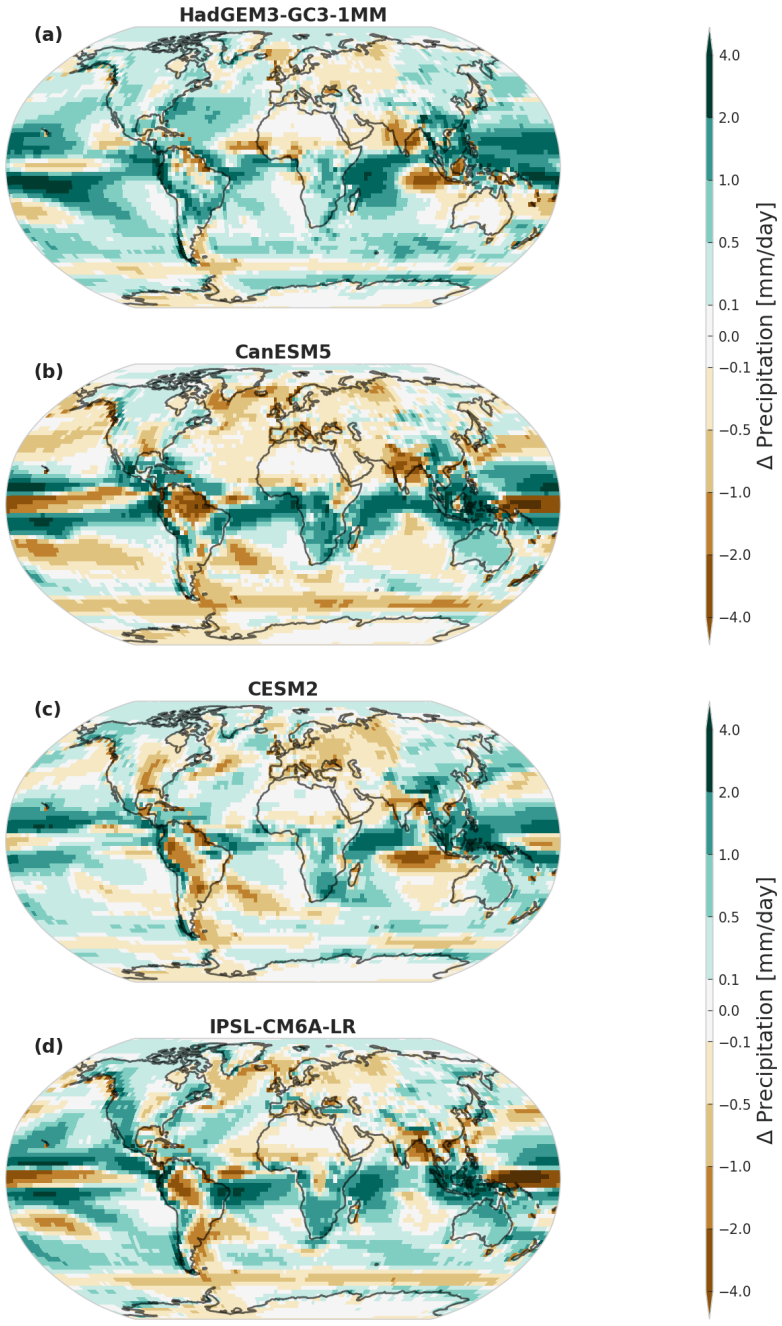

Figure S1. Average precipitation bias (piControl run minus GPCP observations) for the four models: a. HadGEM3, b. CanESM, c. CESM, and d. IPSL. The bias can be as large as the effect of an AMOC collapse over the monsoon regions. In general there is a dry bias over the ISM, wet bias for the EASM and a small dry bias for the WAM. However there is no monsoon region where all models have the same bias, and for the SAM especially they all exhibit distinct patterns. Note that the observational period includes historical forcings which are not present in the piControl.

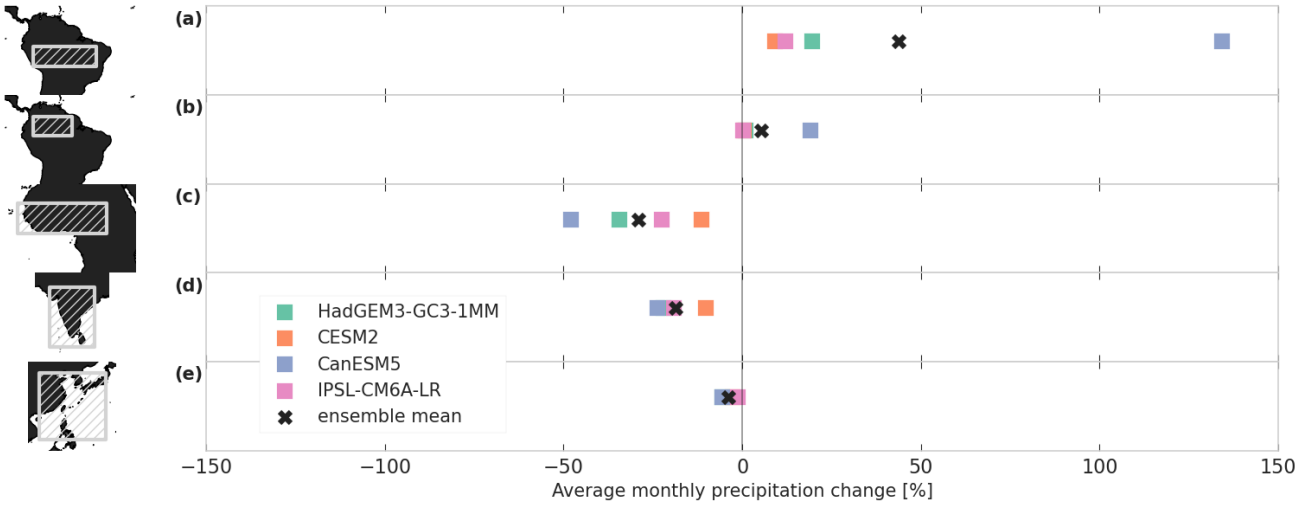

Figure S2. The percentage rainfall change in the land area of five monsoon regions. The first column shows the region for which the precipitation difference is averaged: two parts of the SAM (a,b), as well as in the WAM (c), ISM (d), and EASM (e) (see Table S1). For each model, the x-axis is the average of the 12 individual mean monthly precipitation percentage changes in the region. As well as for the four models (coloured square markers), the ensemble mean is shown (black cross).

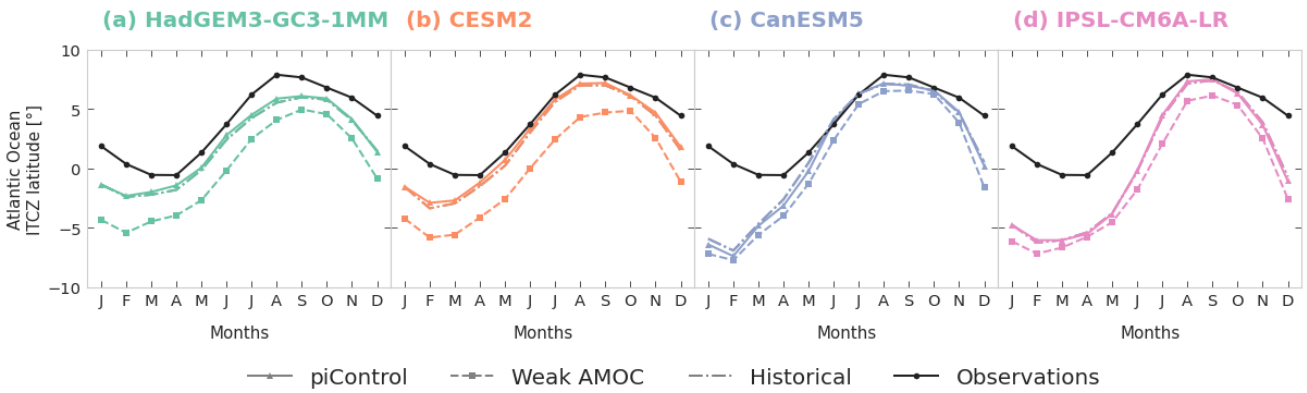

Figure S3. The mean location of the Atlantic ITCZ for each month of the year, before/after AMOC collapse. The observational data is shown in black, the piControl model output in thick coloured lines, the historical runs in dot-dashed coloured lines, and the weak AMOC model output in dashed coloured lines, for a. HadGEM3, b. CanESM, c. CESM, and d. IPSL. See Methods for details.

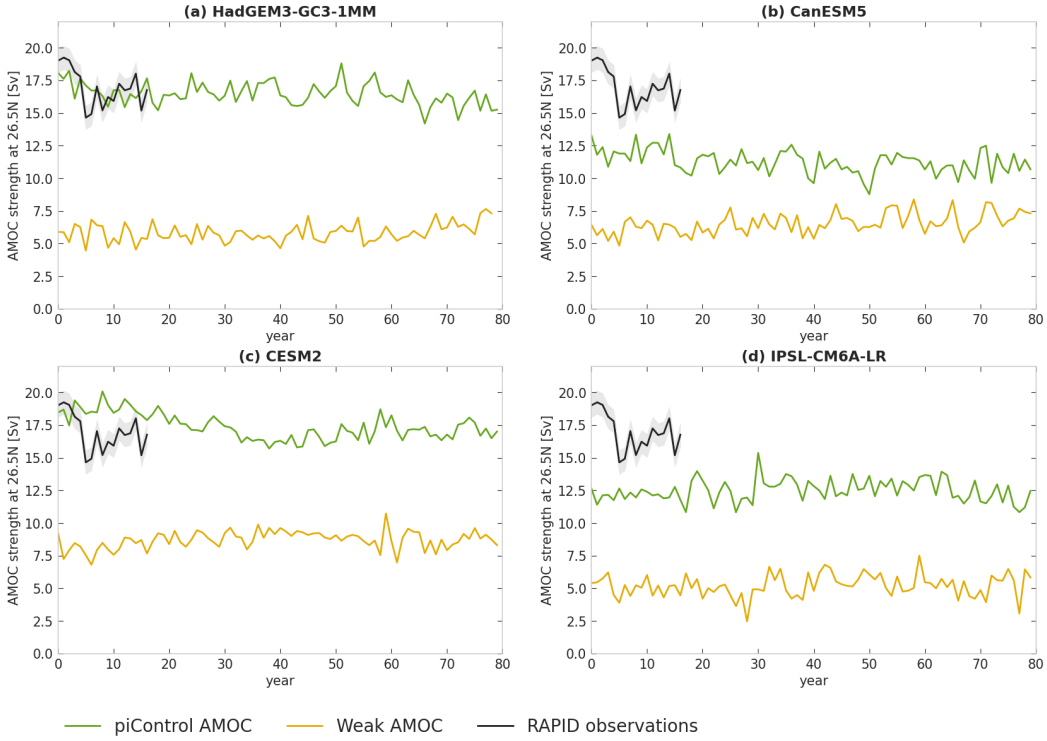

Figure S4. Yearly average AMOC strength at 26.5N for the four model experiments: a. HadGEM3, b. CanESM, c. CESM, and d. IPSL. The piControl strength is shown in solid green and the post-hosing AMOC strength in solid gold. The 4xCO2 AMOC strength is shown in dashed brown. Only the 80 years used in this work are shown. For comparison the RAPID array of AMOC observational measurements from 2004 to 2020 are shown in black with a ±0.9 Sv uncertainty shading. Note, however, that these are historical observations and thus include the effect of anthropogenic forcings, and cannot be directly compared with the piControl simulations. The piControl AMOC is stronger in HadGEM and CESM at about 18 Sv, whilst both CanESM and IPSL have a weaker AMOC at about 12 Sv. The collapsed, weak AMOC has a similar strength in all four models, about 6 Sv, except in CESM2 where its strength is about 8.7 Sv. The 4xCO2 amoc is about the same strength as the collapsed AMOC, except in CESM2 where it is about 2 Sv weaker.

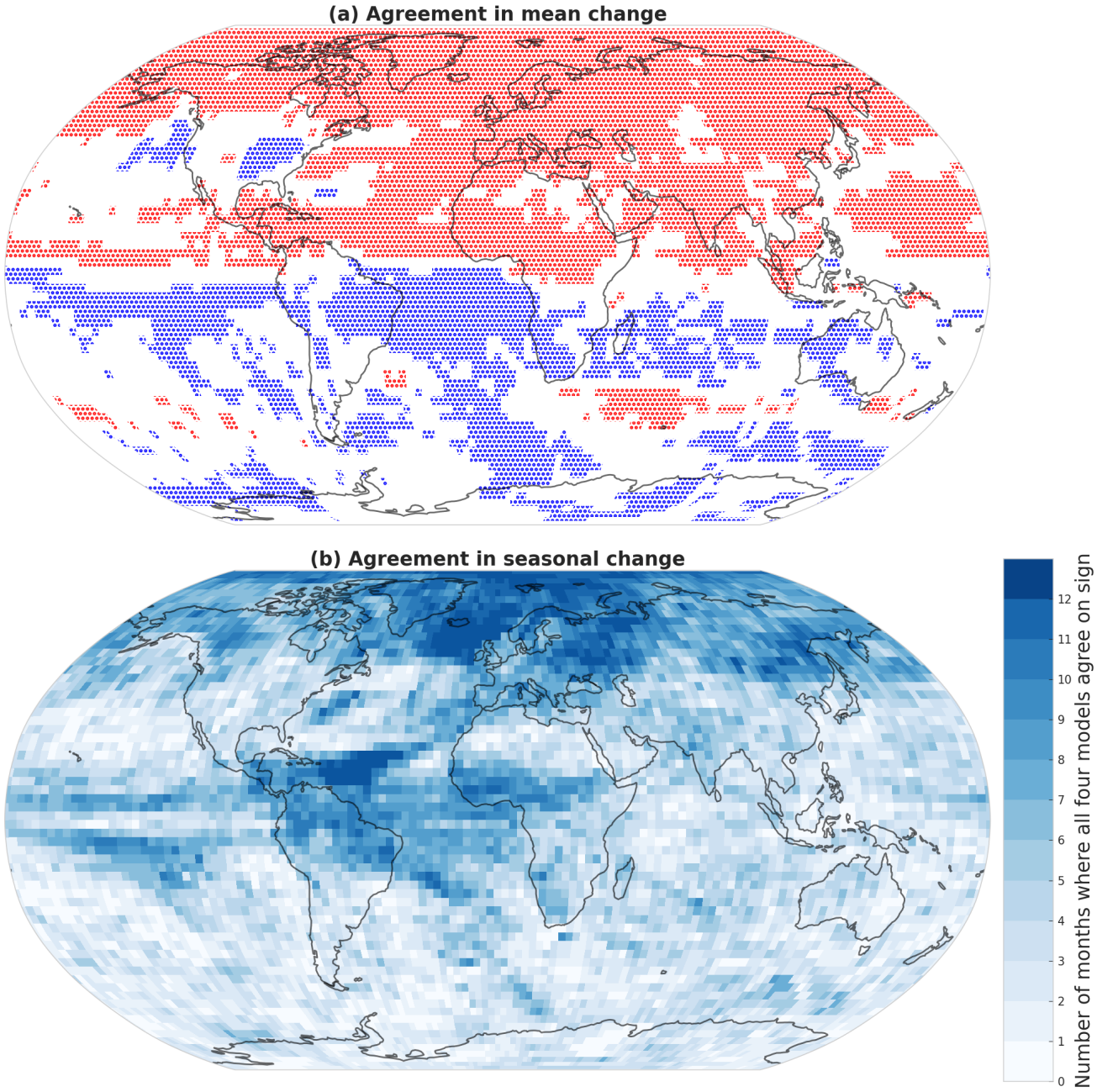

Figure S5. Model agreement in NAHosMIP. (a) The red (blue) stippling indicates the grid-points where all four models agree on the negative (positive) sign of mean annual precipitation anomaly when the hosing experiment is compared with the piControl run. (b) The figures are colored according to the number of months in which the change in the mean monthly rainfall relative to the piControl mean agrees in sign in all four model runs. There is high agreement in the hosing experiments for the SAM and WAM and moderate agreement for the ISM and EASM.

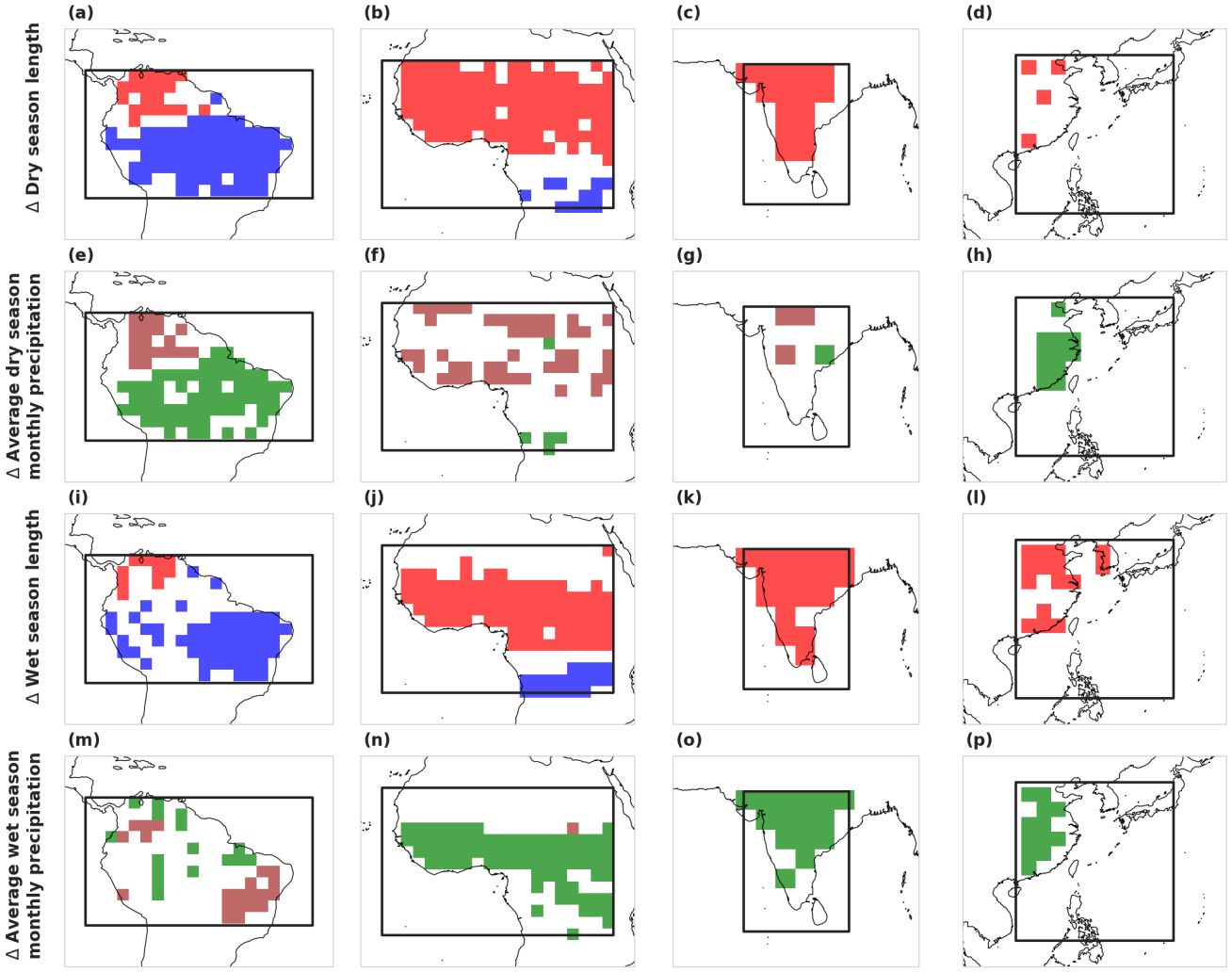

Figure S6. Coloured areas indicate regions of agreement of all four models for the dry and wet season length and precipitation change, as shown in Figure 5 for HadGEM. First row (a-d): blue (red) for shorter (longer) dry season. Second and fourth row (e-h and m-p): green (brown) for a wetter (drier) dry or wet season. Third row (i-l): blue (red) for longer (shorter) dry season. All models agree over the change in dry and wet season lengths over large regions of the SAM, WAM, EASM and ISM. There is less consistent agreement on the sign of the dry and wet season precipitation changes.

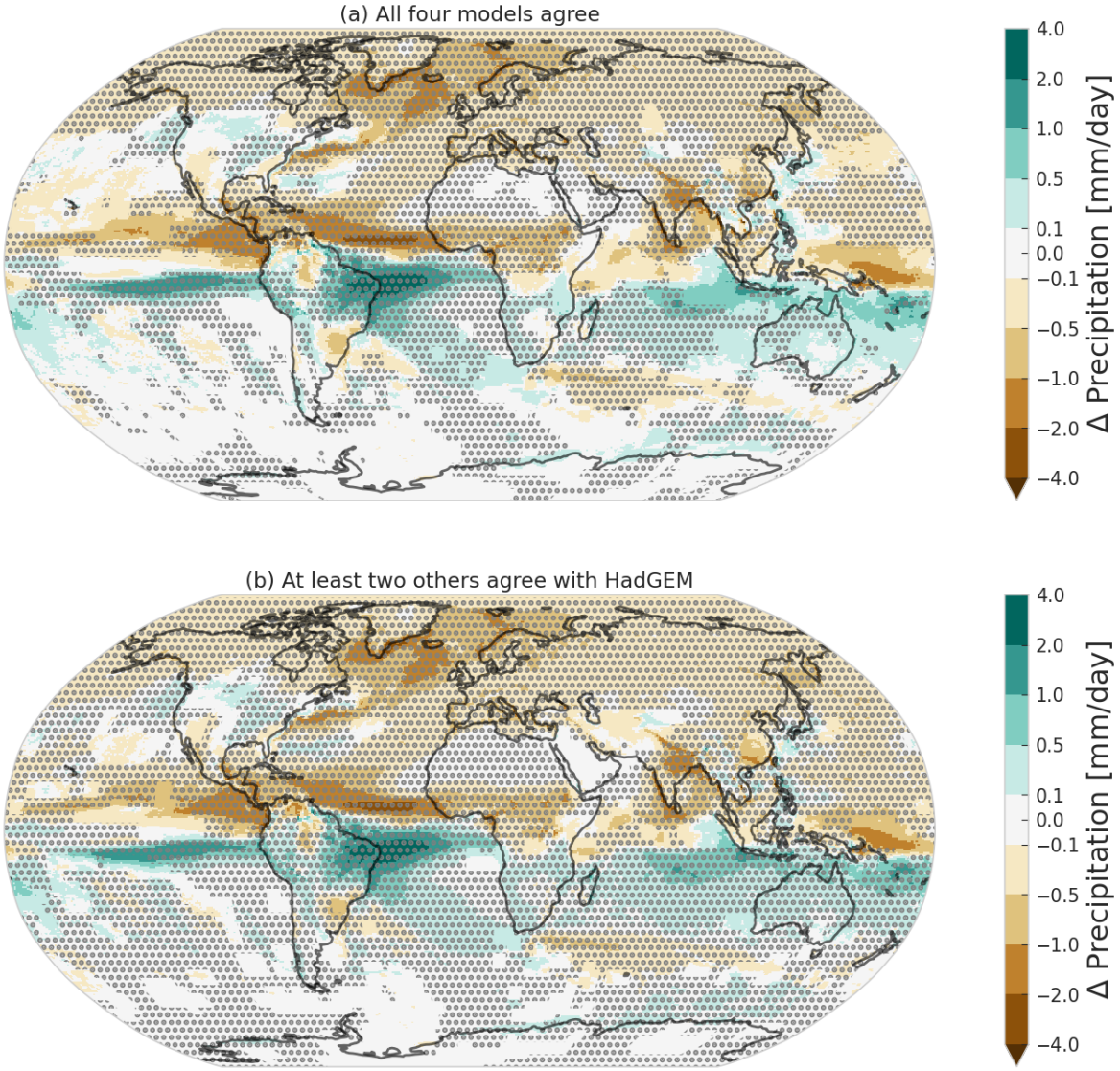

Figure S7. Comparison of the HadGEM precipitation anomaly (weak AMOC minus piControl) with the other model anomalies. In figure (a) the HadGEM precipitation anomaly is plotted and the stippling shows the regions where the sign of the precipitation anomaly in all four models is the same (all four are negative or all four are positive). Figure (b) is the same, but the stippling is in the areas where at least two other model precipitation anomaly signs agree with HadGEM. At least two other models agree with HadGEM over almost the complete monsoon regions, with the exception of the drying of the north-eastern SAM (which is only seen in HadGEM, see Figure 1).

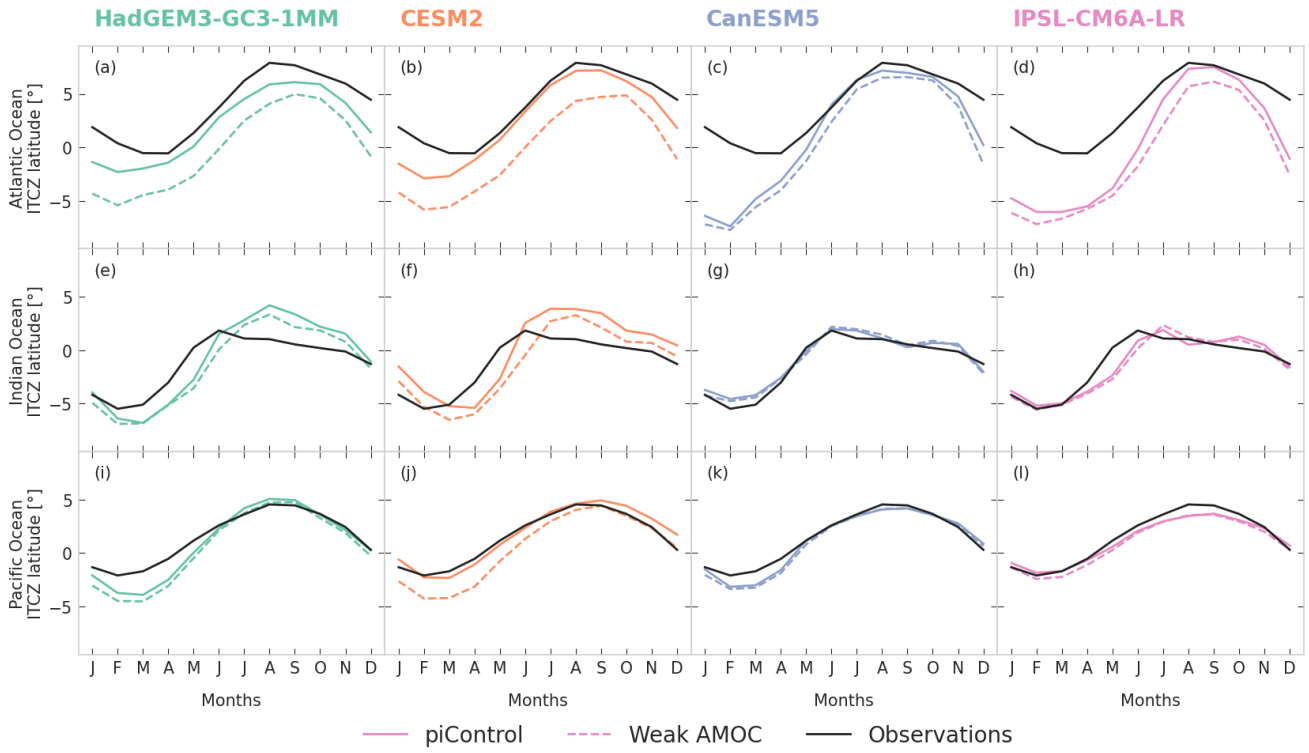

Figure S8. Monthly averages of the ITCZ latitude in the Atlantic (a-d), Indian (e-h) and Pacific oceans (i-l) (see methods). The coloured lines are the piControl (solid) and weak AMOC (dashed) runs. The solid black line shows the observations. All models are close to the observations in the Pacific ocean, and only HadGEM and CESM have a small bias in the Indian. As expected, for all models the Indian and Pacific ITCZs show only a small change after a collapse of the AMOC.

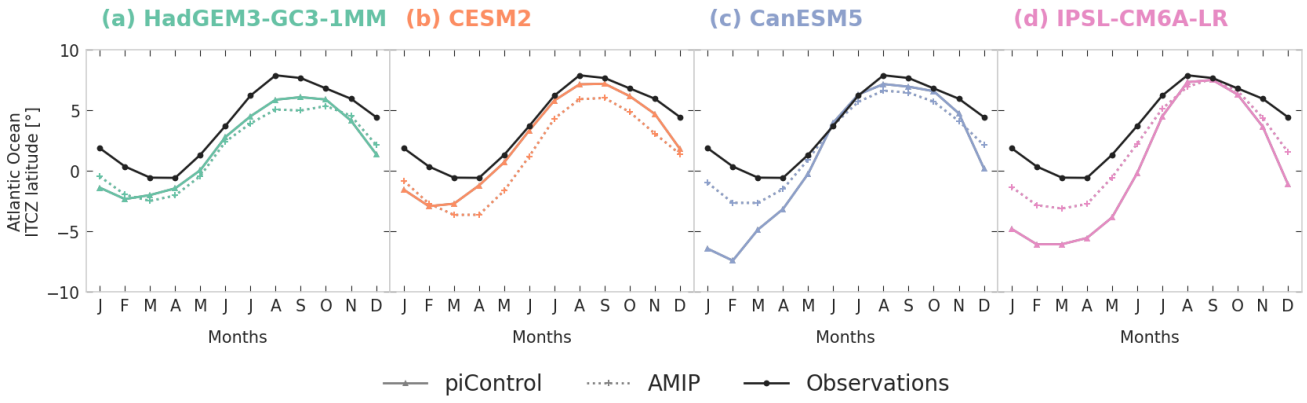

Figure S9. SST bias in the mean location of the Atlantic ITCZ for each month of the year for a. HadGEM3, b. CanESM, c. CESM, and d. IPSL The observational data is shown in black, the piControl model output in thick coloured lines and the AMIP model output in dotted coloured lines. For CanESM and IPSL the AMIP runs have a smaller ITCZ bias, suggesting that part of their Dec-Mar southwardly ITCZ bias is due to SST biases in the models.